Time-resolved methods in Biophysics. 2. Monitoring haem proteins at work with nanosecond laser flash photolysis†

Stefania Abbruzzetti,[a] Stefano Bruno,[b] Serena Faggiano,[b] Elena Grandi,[a] Andrea Mozzarelli[b] and Cristiano Viappiani*[a]

Received 18th July 2006, Accepted 25th September 2006
First published as an Advance Article on the web 18th October 2006
DOI: 10.1039/b610236k

Haem proteins have long been the most studied proteins in biophysics, and have become paradigms for the characterization of fundamental biomolecular processes as ligand binding and regulatory conformational transitions. The presence of the haem prosthetic group, the absorbance spectrum of which has a ligation sensitive region conveniently located in the UV-visible range, has offered a powerful and sensitive tool for the investigation of molecular functions. The central Fe atom is capable of reversibly binding diatomic ligands, including O_2, CO, and NO. The Fe-ligand bond is photolabile, and a reactive unligated state can be transiently generated with a pulsed laser. The photodissociated ligands quickly rebind to the haem and the process can be monitored by transient absorbance methods. The ligand rebinding kinetics reflects protein dynamics and ligand migration within the protein inner cavities. The characterization of these processes was done in the past mainly by low temperature experiments. The use of silica gels to trap proteins allows the characterization of internal ligand dynamics at room temperature. In order to show the potential of the laser flash photolysis techniques, combined with modern numerical analysis methods, we report experiments conducted on two non-symbiotic haemoglobins from *Arabidopsis thaliana.* The comparison between time courses recorded on haemoglobins in solution and encapsulated in silica gels allows for the highlighting of different interplays between protein dynamics and ligand migration.

Introduction

The rebinding of ligands to haem proteins in solution following laser photolysis has been extensively used over the years to understand the molecular mechanisms underlying protein–ligand interactions. A very useful property of haem–carbon monoxide complexes is that they are easily photodissociated by visible light, which cleaves the Fe–ligand bond without side reactions. The difference in the absorbance between the carboxy and the deoxy species can be exploited to monitor the time evolution of the rebinding reaction. As the ligand quickly rebinds to the haem, photolysis can be cycled and signal averaging can be performed. After dissociation from the haem iron, ligands either rebind from the protein inner cavities in the so-called geminate recombination, or escape into the solvent through exit channels. The observed rebinding kinetics results from the combination of protein dynamics and ligand migration within the protein matrix.

[a]*Dipartimento di Fisica, Università degli Studi di Parma, Parma, Italy. E-mail: cristiano.viappiani@fis.unipr.it; Fax: +390521905223; Tel: +390521905208*

[b]*Dipartimento di Biochimica e Biologia Molecolare, Università degli Studi di Parma, Parma, Italy*

† Edited by J. Nield. This paper is derived from the lecture given at the X School of Pure and Applied Biophysics "Time-resolved spectroscopic methods in Biophysics" (organized by the Italian Society of Pure and Applied Biophysics), held in Venice in January 2006.

An impressive number of experimental studies have characterized the rebinding kinetics under a variety of experimental conditions for myoglobin (Mb),[1–15] haemoglobin (Hb)[12,16–25] and, more recently, to other haem proteins as, for instance, neuroglobin.[26,27] The recent exploitation of protein encapsulation in wet nanoporous silica gel,[28] possibly in the presence of increased viscosity by added cosolvents as glycerol, has offered a powerful new tool to study the coupling of protein dynamics and ligand migration at room temperature, thus opening exciting new perspectives. The increased viscosity of the medium, the confinement effect in the gel pores and the presence of allosteric effectors affect, to a different extent for each protein, the dynamics of the macromolecule, thus allowing the trapping of unstable states (*e.g.* by dramatically slowing down ligation-dependent tertiary and quaternary transitions) and unveiling ligand migration pathways even at room temperature. In the case of human haemoglobin (HbA), these studies have supported the Tertiary Two State model, an extension of the classic MWC allosteric model.[29] Furthermore, the judicious use of model-independent lifetime distributions associated with ligand rebinding and numerical modelling of the rebinding kinetics allowed the retrieval of microscopic rates for the elementary processes, that were interpreted on the basis of structural models.[30–32] Similar approaches have been applied to Mb[33–35] and two truncated Hb.[34] The influence of the gel on the ligand binding reaction is mostly evident in the geminate phase, as protein dynamics is expected to play a fundamental role in

Stefania Abbruzzetti

Stefania Abbruzzetti graduated cum laude *at the University of Parma, Italy, and her dissertation won an award (1996) from the Italian Biophysical Society (SIBPA). She obtained her PhD from the same institution in 2001. From then on, she has been a postdoctoral research fellow at the University of Parma. Her work focuses on the study of functional and structural dynamics in proteins, investigated by laser flash photolysis. The main research topics are the photochemical characterization of caged compounds and their use in protein folding problems, and the study of functional properties in haem proteins.*

Stefano Bruno

Stefano Bruno received his degree in pharmaceutical chemistry cum laude *from the University of Parma in 1997 and his PhD from the University of Turin in 2002. After a post-doc fellowship at the Department of Biochemistry of the University of Oxford in 2002–2004, he is now Researcher at the University of Parma in the Department of Biochemistry and Molecular Biology. His research interests include experimental studies of haem proteins in solution, in the crystalline state and immobilized in nanoporous silica gels, using several spectroscopic techniques, both time-resolved and steady state.*

Serena Faggiano

Serena Faggiano was born in 1979 in Bari, Italy. She was awarded the status of best student of her course for the year 1999 and she received her degree cum laude *in pharmaceutical chemistry from the University of Parma in 2005. She is currently a PhD student in the Department of Biochemistry and Molecular Biology at the University of Parma. Her work focuses on the study of haem proteins, with a particular interest in hexacoordinated haemoglobins and haemoglobin-based blood substitutes.*

Elena Grandi

Elena Grandi was born in 1978 in Modena, Italy. She received her degree cum laude *in physics from the University of Parma in 2004. She is currently working as a PhD student in the Department of Physics at the University of Parma, where she studies fast kinetics in plant haemoglobins and GFP mutants.*

Andrea Mozzarelli

Andrea Mozzarelli received his degree in chemistry in 1974. He is Full Professor of Biochemistry at the Faculty of Pharmacy, University of Parma, Parma, Italy. His main research interest is the elucidation of structure–dynamics–function relationships of hemoglobins, pyridoxal 5-phosphate-dependent enzymes and green fluorescent proteins. Protein immobilization via crystallization or encapsulation in wet, nanoporous silica gels has been exploited as a novel tool to select and isolate distinct tertiary and quaternary conformations, analyzed by spectroscopic and microspectroscopic methods. Advanced computational methods are applied to determine free energy of ligand–protein interactions and to predict the affinity of designed protein ligands.

Cristiano Viappiani

Cristiano Viappiani is Professor in Applied Physics at the Faculty of Pharmacy of the University of Parma, where he received his PhD in physics in 1993. His research activity is mainly concerned with the use of nanosecond laser based techniques, including time-resolved photoacoustics and nanosecond transient absorbance, to investigate protein structural dynamics and function. He has recently introduced laser induced pH-jump techniques to the field of protein folding and is actively working on the development and photochemical characterization of photolabile caged compounds. His interests include the dynamics of immobilized haem proteins using laser flash photolysis.

opening escape routes from the primary docking site within the distal pocket. For instance, very little effects are observed in the geminate phase of HbA,[36] while a very remarkable increase in the extent of this phase is observed for Mb.[36,37]

The presence of hydrophobic cavities has emerged recently as an important factor in determining ligand internal dynamics and reactivity.[38] For instance, in the case of Mb, ligand rebinding kinetics for different mutants and under Xe pressures[39–41] suggested that the dissociated ligand may migrate to a hydrophobic cavity, called Xe1 cavity,[42] on the proximal side of the haem, possibly *via* the Xe4 cavity on the distal side.[38] This has allowed for the rationalizing of the inverse temperature effect observed in the geminate phase at low temperatures, which was previously attributed to a glassy behaviour of the protein. Low temperature X-ray crystallography studies[43–45] have located the dissociated CO in these cavities, whereas time-resolved X-ray crystallography studies have followed, in real time, the ligand rebinding, ligand migration, and associated protein structural changes.[46–49] More recently, cavities have been postulated to be involved in the metabolism of NO in Mb,[38,50] neuroglobin,[51] and truncated haemoglobins.[52] These peculiar structural features have profound effects on the ligand binding kinetics.[27,34]

The laser flash photolysis method is thus undergoing renewed interest in the investigation of protein dynamics and ligand migration, due to a favourable combination of state of the art instrumentation with laser-limited time resolution and protein entrapment into metastable states. In this work we provide an introduction to state of the art nanosecond laser flash photolysis methods, presenting applications to the study of ligand binding kinetics to two recently discovered non-symbiotic haemoglobins from *Arabidopsis thaliana* (termed AHb1 and AHb2) trapped into wet, nanoporous silica gels. It is beyond the scope of this paper to cover the whole spectrum of applications in photochemistry and photobiology, which are discussed in several published reviews (see, *e.g.* ref. 53 and 54).

Principles of the method

Nanosecond time-resolved absorption techniques rely on the use of a probe beam that interrogates the sample before and after excitation with a nanosecond laser (laser flash photolysis). The general principles of the method are covered in recent reviews,[53,54] some of which put special emphasis on the applications to proteins.[12,55] These techniques allow, in general, the study of both the disappearance of the originally formed transients as well as the formation of new species. The probe beam is most generally a broadband, cw light source in the UV-vis-NIR spectral range, where transient electronic transitions are probed. The near UV-violet spectrum is of special interest, as the so-called Soret band of the haem is located in this region. The interest stems from the remarkable sensitivity of this absorption band to the ligation state of the haem Fe as well as to changes in the surrounding structure.

The experimental parameter of interest is a change in absorbance (ΔA), reflecting changes in transmitted light from the probe beam before, $I(t < t_0)$, and after, $I(t)$, laser excitation, according to the following equation: $\Delta A\,(t) = -\log \frac{I(t)}{I(t<t_0)}$

The instrumental outline is summarized in Fig. 1, where a collinear pump/probe geometry is presented. Due to the geometrical configuration of the gel-embedded samples, which are thin (≈0.1–1 mm) slabs deposited on an optical quality silica surface, with an absorbance of ≈1 in the Soret region, it is mandatory to work with (almost) collinear pump and probe beams to optimize the overlap between the two beams and to obtain a homogeneous excitation of the probed volume. Fig. 1 presents two different experimental layouts, which will be discussed below.

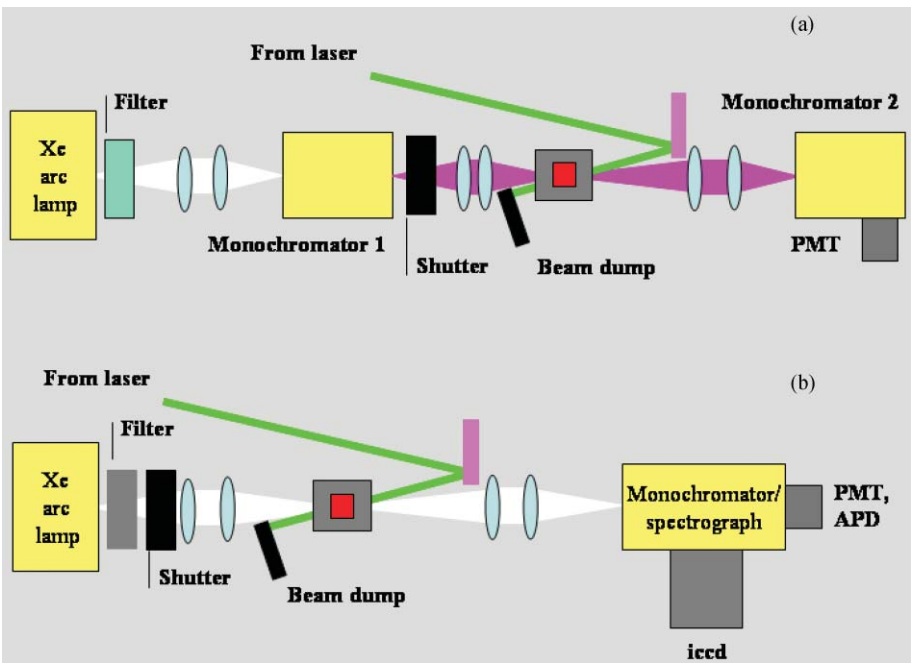

Fig. 1 Experimental layout for the nanosecond laser flash photolysis setup with (a) monochromatic and (b) white light detection beams.

Laser flash photolysis setup

There are two basic configurations used in our laboratory, outlined in Fig. 1, which allow versatile and sensitive detection of single wavelength transient absorbance traces or time-resolved spectra with laser limited time resolution.

A convenient photolysis source for photolysis of CO complexes of haem proteins is the second harmonic (532 nm) of a Q-switched Nd:YAG laser. In our setup we use either a Surelite II-10 (Continuum) or a Handy Yag HYL-101 (Quanta System). The linear polarization is converted to circular by means of a quarter waveplate in order to minimize photoselection effects. Near-full photolysis is normally obtained with the setups described below, with laser pulses of 20–40 mJ, depending on the sample. The need for pursuing full photolysis conditions is simply due to the requirement of working with known concentrations of reactants (deoxyhaem and CO) for quantitative analyses. The use of gels removes the additional complications in the kinetics arising from switching between ligation dependent conformational states. For instance, the R to T transition, normally observed when full photolysis of COHb is performed in solution, is completely inhibited when COHb is trapped in the gel.[36]

In the setup described in Fig. 1(a), the absorbance changes are monitored using a monochromatic cw output of a 150 W Xe arc lamp coupled to a 0.25-m monochromator (AMKO gmbh). The transient absorbance traces are measured through a second, 0.125-m monochromator (77250, LOT-Oriel) with a 5 stage photomultiplier (PMT) (Applied Photophysics). The voltage signal is digitized by a digital oscilloscope (LeCroy LT374, 500 MHz, 4 GS s^{-1}; LeCroy 9370, 1 GHz, 1 GS s^{-1}). A custom dichroic filter (Omega optical) is positioned between the exit slit of the monochromator and the photomultiplier to remove the residual stray light from the pump laser. A fast shutter (Vincent Associates, Uniblitz VS35) is positioned between the output of the first monochromator and the sample holder. The opening of the shutter is controlled by a dedicated microprocessor,[56] while exposure time is set by the shutter driver (Vincent Associates, Uniblitz VMM-T1). The sample holder is accurately temperature controlled with a Peltier element, allowing a temperature stability of better than 0.1 °C.

A second setup is outlined in Fig. 1(b),[57] where the cw output of a 75 W Xe arc lamp is focused onto the sample holder, then collimated and finally entered into the entrance slits of a MS257 (LOT-Oriel) monochromator/spectrograph. With this versatile setup, time-resolved difference absorbance spectra can be measured using the on-axis exit port of the MS257 spectrograph, to which a gated intensified CCD (Andor Technology, iStar DH734, 1024 × 1024 pixels) was coupled. The intensified CCD (iCCD) is normally operated in the full vertical binning mode and the spectra measured with a gating time of 2.93 ns. Also in this setup, a fast shutter (Vincent Associates, Uniblitz VS35) is positioned between the output of the Xe lamp and the sample holder. We normally measure time-resolved spectra consisting of photoproduct minus AHbCO difference spectra at various time delays following photodissociation. Depending on the time span, 100 to 120 logarithmically spaced spectra are measured to cover the complete time course of the CO rebinding kinetics, from 10 ns after the laser flash to 0.1 s. Spectra are obtained by averaging 100 single shot signals at each delay. Synchronization of the overall experiment (laser firing, shutter opening, and iCCD triggering) is achieved by means of dedicated hardware.[56]

The off axis port of the MS257 is used to monitor single wavelength kinetics. The monochromatic light is collected from the exit slit by dedicated optics after being passed through a custom dichroic filter (Omega optical) and focused onto a Si APD (Hamamatsu S2382) coupled with a transimpedance amplifier (Avtech AV149, 600 MHz). The light intensity which is available in single monochromator applications is high enough to allow the use of photodiode detectors. Also for this setup, the voltage signal is digitized by a digital oscilloscope (LeCroy LT374, 500 MHz, 4 GS s^{-1}; LeCroy 9370, 1 GHz, 1 GS s^{-1}).

Repetition rate is a relevant parameter of the experiment as the sample must fully recover between laser flashes. Thus, depending on the sample, repetition rates as low as 0.1 Hz could be necessary.

Detectors

Many detectors are nowadays available which allow to reach nanosecond resolution, provided optimal conditioning electronics is used. Side-on PMTs (photomultiplier tubes) with 5 stages wired[54] are the detectors traditionally used in nanosecond laser flash photolysis setups and are the only detectors with the necessary sensitivity in setups with two monochromators (Fig. 1(b)). When exposure of the PMT to the intense monitoring light is limited to a few hundred ms, these detectors can withstand currents of 2–4 mA without showing fatigue.[58] These currents result in 100–200 mV signals when fed into the 50 Ω load of a digital oscilloscope, without the need for an intervening amplification, and thus preserving maximum signal bandwidth. In addition, modern oscilloscopes have very low capacitance (typically <20 pF), which results in RC values allowing nanosecond resolution. Time scales longer than a few hundred ms can be accessed by limiting the PMT currents (*e.g.* using lower light intensity), and using higher loads.[54]

Preamplified positive-intrinsic-negative (PIN) and avalanche Si photodiodes (APD) are an option for setups where a single monochromator is used as in Fig. 1(a). We have shown in several papers that this detection system is reliable and sensitive enough for transient absorption application with nanosecond resolution from the near UV to the near infrared (see *e.g.* ref. 37,57,59–62).

In the past, pulsed Xe arc lamps were used to reach the nanosecond time scale. However, with state of the art detectors and electronics it is no longer necessary to resort to such light sources, and cw Xe lamps are the sources of choice for general purpose applications. The 75 W Xe lamp is the best performing lamp if we consider the irradiance of its image at the entrance slit of the monochromator.[54] Depending on the optical layout and the detector in use, Xe lamps allow to determine transient absorbance traces between 250 and 900 nm. Wavelengths below 390 nm are essentially still inaccessible to photodiodes (on the nanosecond time scale), while they allow very sensitive detection in the near infrared. While the use of shutters to limit the exposure time is unavoidable for photomultipliers, it is strictly not necessary for photodiodes, which can withstand mA currents for very long times. Nevertheless, it is convenient to shutter the monitoring beam to limit the amount of white light shining on the sample, thus preventing photoinduced damage.

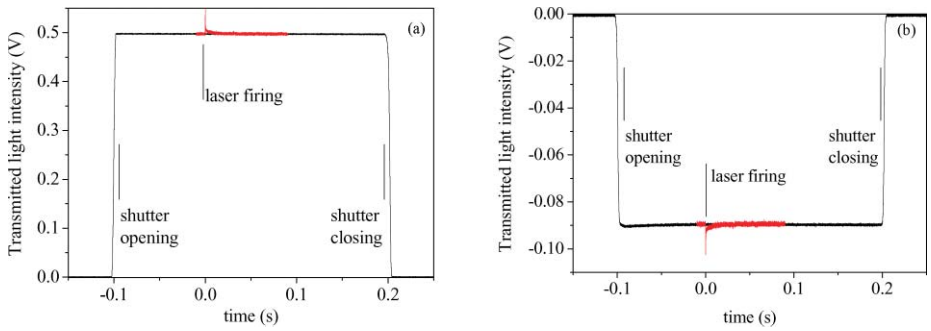

Fig. 2 (a) Transmitted light intensity at 436 nm as monitored by a Si APD. The shutter is opened 100 ms before the laser fires. The opening of the large aperture shutter requires about 10 ms and quickly settles to a stable value until the monitoring shutter is closed. The light level before the laser fires determines the value of $I(t < t_0)$ in eqn (1). The change in transmitted light intensity is shown (on a $\times 2$ scale) as the red signal superimposed on the black curve. (b) Transmitted light intensity at 436 nm as monitored by a 5 stage PMT. Note the negative sign of the measured voltage and the small overshoot after opening of the shutter, which recovers within 100 ms. The signal (red trace shown on a $\times 3$ scale) is acquired in the flat region starting at 100 ms after the laser flash.

It is worthwhile to comment on the time profile of the PMT output current. The use of Xe lamps requires shutters with large areas to allow for maximum light throughput when open. However, this results in opening times of the order of a few ms. Therefore, the current rises slowly following the opening of the shutter and, then, has normally an overshoot, eventually settling to a stable, steady state value within 50–100 ms. Thus, it is necessary to wait $\approx$100 ms after opening of the shutter, before firing the laser. This concept is illustrated in Fig. 2(a), where the time course of the voltage drop across the 50 Ω load of the digital oscilloscope is shown. A visual comparison with the voltage signal measured by a Si APD immediately highlights a major advantage of the latter detection system, for which a steady state is quickly reached after the shutter is opened, without any sign of overshooting.

Time resolution of the method

The finding of ligand migration signatures in the absorbance change on the nanosecond time scale after photolysis of immobilized systems[32,33,63] calls for laser-limited time resolution in any experimental setup which is intended for ligand binding studies. The time resolution is in principle set by the laser pulse width, which, for modern solid state lasers, is normally around 5 ns. Nevertheless, there are a number of parameters influencing the actual time resolution, that need to be discussed.

Several parameters and experimental details contribute to the overall bandwidth of the detection systems and affect the access to the short time scale after laser excitation. A critical issue in determining time resolution is the intense light scattering from the pump source, which is generated when the light pulse hits the gel slab. For this reason, it is necessary to work with counter-propagating pump and probe beams. No matter how careful the alignment is, a relevant portion of the pump light is scattered towards the detector. Reduction of the scattered light is obtained with a careful positioning of the optical components, and the insertion of one or more beam dumps to block reflections from the optics, including the cuvette walls. The use of a monochromator in front of the detector is essential to reduce the scattered pump light to reasonable levels. Even so, some residual stray light may reach the detector, and for this reason it is strongly advisable to place a dichroic mirror after the exit slit of the monochromator. Fluorescence emission from haem photoexcitation is negligible and, contrary to what generally occurs with most organic molecules, this does not constitute a problem in impairing time resolution.

Provided laser scatter is efficiently rejected, time resolution is determined by the overall electronic bandwidth of the detection system, as detailed in the previous section. Each component of the detection chain is critical if laser limited nanosecond resolution is the target of the setup.

The signals we are interested in are generally extended in time over several orders of magnitude. Thus, the voltage must be sampled at a high sampling rate for the first few microseconds following the nanosecond excitation, in order to reconstruct the fast kinetics with the appropriate resolution. To monitor in a single shot both the fast and the slow parts of the kinetics under investigation, it would be necessary to sample the signal at high rate for a long time, reaching the 0.1 s time scale. This would require the use of expensive digitizers equipped with long memories. Although digital oscilloscopes are available today with very deep memories, the mass of acquired data is redundant at long times, and is a useless waste of data storage space.

If the acquisition memory of the oscilloscope is limited, acquisition of the signal at several time bases is necessary to cover the whole time course. This has the drawback of requiring longer acquisition times and sometimes leads to photodegradation of the samples, due to the extensive photolysis. In addition laser pulse energy fluctuations often result in signals with different amplitudes needing to be rescaled with sometimes difficult to determine scaling factors. An alternative option is the use of exponentially increasing delays in the data acquisition system.[56,64]

Signals shown in Fig. 2 are normally acquired using a digital oscilloscope. Modern digital oscilloscopes are normally capable of acquiring data at sampling rates exceeding 1 GS s^{-1}, with analog bandwidth of 500 MHz. The vertical resolution of the ADC is 8 bit in the single acquisition mode, requiring amplification of the signal and application of an offset. Both functions are nowadays available on the digital oscilloscope. In order to improve the signal to noise ratio, the kinetic traces are typically averaged over 100 laser shots. In this process, the random noise is strongly reduced and the vertical resolution is effectively increased.

Data analysis

Analysis of time-resolved spectra

Difference spectra calculated from the kinetics series by subtracting the spectrum of the CO-form at equilibrium are normally analysed by singular value decomposition (SVD).[65] The SVD analysis reported in this paper was performed using the software MATLAB (The Mathworks, Inc., Natick, MA). Our data matrix, $\boldsymbol{D}$, consists of difference absorbance measured as a function of two variables: the wavelength of the probe beam and the time delay between the photolysis beam and the opening of the gate of the CCD image intensifier. The singular value decomposition of $\boldsymbol{D}$ can be written as:

$$\boldsymbol{D} = \boldsymbol{USV}^{\mathrm{T}} \tag{1}$$

where the columns of $\boldsymbol{U}$ are a set of linearly independent, orthonormal basis spectra, the columns of $\boldsymbol{V}$ describe the time-dependent amplitudes of these basis spectra, $\boldsymbol{V}^{\mathrm{T}}$ indicates the transpose of matrix $\boldsymbol{V}$, and the matrix $\boldsymbol{S}$ is a diagonal matrix of non-negative singular values which describe the magnitudes of the contributions of each of the outer products of the i-th column vectors $U_i V_i^{\mathrm{T}}$ to the data matrix $\boldsymbol{D}$.[65]

Most of the higher order components of the SVD contain no real spectral information and correspond to noise with a random time dependence. A first criterion for the selection of usable components is the magnitude of the singular values, the higher values being the meaningful ones. The selected components can be further screened by evaluating the autocorrelations of the corresponding columns of $\boldsymbol{U}$ and $\boldsymbol{V}$ and rejecting the component if either autocorrelation falls below 0.8.[65] In the experiments reported in this paper, only the first two components were retained for further analysis. The time course of the Vs is then analysed with a proper kinetic model.

Analysis of ligand binding kinetics

Ligand binding kinetics following nanosecond laser photolysis reflects the ligand migration inside the protein matrix and the reactivity towards freely diffusing molecules. Although O_2 is the physiological ligand of Mb and Hb, it is often difficult to avoid irreversible oxidation or side reactions while studying these very reactive species *in vitro*. In model studies, carbon monoxide (CO) is often preferred to oxygen as a ligand, since chemical reactions subsequent to binding of the ligand are prevented. CO generally binds even more strongly than O_2 to the haem and its complexes are extremely stable on the long term. The Fe–CO bond is photolabile and the use of short (nanosecond) light pulses allows to prepare a state in which a large population of reactive deoxy states can be then be monitored spectroscopically as it binds CO over time. The time span of this process is generally extended over several orders of magnitude in time. Immediately after the end of the laser pulse, the ligand undergoes competitive reactions, in which it can either move through the protein matrix and may be temporarily docked into hydrophobic pockets, or react with the haem to form the carboxy adduct. This short time scale phase is generally called geminate recombination and is independent of reactant concentrations. Competition of the internal reactions with the escape of the ligand to the solvent results in a fraction of deoxy-haems surviving on the microsecond time scale. These molecules react with the freely diffusing ligands in a bimolecular reaction which may extend to the milliseconds, with a concentration dependent rate. In a typical experiment, the concentration of the protein is below 100 μM, while the solubility of CO affords a concentration on the order of 1 mM at 1 atm and 293 K, leading to pseudo-first order reactions. Experiments at different CO concentrations are normally performed to distinguish between geminate (concentration independent) and bimolecular (concentration dependent) phases. If multimeric proteins with allosteric properties are investigated, as is the case of the tetrameric human Hb, the ligand binding is overlapped to a conformational switching, affecting the rate constants for the ligand binding reactions. This results in very complex kinetics which are difficult to model. The use of silica gels to trap conformational states has allowed disentangling the ligand binding after laser flash photolysis from the conformational switching, thus simplifying dramatically the ligand binding kinetics.

The existence of kinetic heterogeneity due to structural and dynamic sources is a well known problem in the analysis of ligand binding progress curves. Structural relaxation and ligand migration through discrete docking sites lead sometimes to complex kinetic patterns, which are difficult to model. In the case of myoglobin, an integrated approach was successfully applied to the quantitative analysis of CO rebinding curves.[33,66]

An extremely powerful approach is the determination of model independent lifetime distributions using the Maximum Entropy Method (MEM), a mathematical algorithm based on information theory.[67,68] A model-independent lifetime distribution, $g(\log(\tau))$, associated with the observed kinetics is evaluated using the MEM, in terms of which the observed kinetics can be expressed as:

$$N(t) = \int_0^\infty g(\log\tau)\, \mathrm{e}^{-\frac{t}{\tau}}\, \mathrm{d}(\log\tau) \tag{2}$$

The use of the MEM affords lifetime distributions that can be sometimes analysed in terms of sum of Gaussian shapes to retrieve average lifetimes.[30,31,41] This is of special interest when the reaction scheme allows the determination of the analytical solution of the associated system of coupled differential equations. In this case, the microscopic rates can be extracted from the apparent (average) rates determined from the analysis of the MEM distributions.[30–32,55]

We have recently demonstrated that in some cases the application of relatively simple kinetic models can reproduce surprisingly well the ligand rebinding kinetics for MbCO and HbCO gels.[31,32,69] Apparently, under specific conditions the use of reactions schemes where single rate constants are used, instead of lifetime distributions (as for the case of the MEM analysis), gives a reasonable description of the kinetics. This was particularly true for the case of AHb1 and AHb2 solutions, for which very good fits to CO rebinding kinetics could be obtained in the whole temperature and CO concentration ranges that were investigated.[69] Some misfit was found on the long time tail of the CO rebinding kinetics to Mb and Hb silica gels, suggesting that for these samples the structural heterogeneity and/or long time scale structural relaxations are affecting the rebinding curve.[31,32]

The definition of the reaction scheme can benefit from the determination of time-resolved spectra, as this facilitates the identification of reaction intermediates. In the case of the non-symbiotic haemoglobins AHb1 and AHb2 from *Arabidopsis thaliana* reported in this paper, the competition between the

endogenous (His) and the exogenous (CO) ligand leads, in a fraction of the photodissociated molecules, to formation of a transient hexacoordinated species, in which the sixth position of the haem Fe is temporarily occupied by the internal His ligand. Eventually, this species will disappear as CO binds to the haem. The subtle changes in the absorption spectrum accompanying the change from five coordinated high spin (5c-HS) to six coordinated low spin (6c-LS) can be exploited to monitor this reaction.

Samples preparation

AHb1 and AHb2 were cloned, expressed and purified as described elsewhere.[69]

For experiments in solution, the concentrated stock solutions of either AHb1 or AHb2 were diluted in 100 mM sodium phosphate buffer, 1 mM EDTA, pH 7.0 to a final concentration ranging from 60 to 70 μM. Before the experiments, the solutions were equilibrated with nitrogen–CO mixtures of known CO partial pressure and sodium dithionite was added to a concentration of 2 mM to prevent oxidation.

The encapsulation of both AHb1 and AHb2 in silica gels was carried out following the protocol reported by Shibayama and Saigo[70] with some modifications. A solution containing tetramethyl orthosilicate, water and hydrochloric acid was sonicated for 20 min at 4 °C. An equal volume of a deoxygenated solution containing 10 mM phosphate at pH 6.0, was then added to the sol, which was further deoxygenated for 40 min at 4 °C under flux of nitrogen. Finally, a 200 μM solution of either AHb1 or AHb2 in a 50 mM phosphate buffer at pH 7.2 was anaerobically added to the sol. The resulting mixture was layered on quartz plates under anaerobic conditions. Gelation occurred in approximately 20 min. The silica wet gels were anaerobically stored in a buffer containing 100 mM phosphate, 1 mM EDTA, 5 mM sodium dithionite at pH 7.0. Before the experiments, the gels were soaked in a solution previously equilibrated with a CO–nitrogen mixture of known CO partial pressure.

Ligand binding to AHb1 and AHb2 from *Arabidopsis thaliana*

The effect of the gel structure on the ligand binding kinetics is strongly dependent on the protein structure

The interplay between ligand migration and protein relaxation is becoming a relevant issue in connection with the mechanistic aspects of protein function. We have recently investigated the ligand binding properties of two non-symbiotic haemoglobins from *Arabidopsis thaliana*, termed AHb1 and AHb2.[69] Using resonance Raman and absorption spectroscopies, we showed that Fe^{2+}AHb1 contains a mixture of pentacoordinated high-spin (5c-HS) and hexacoordinated low-spin (6c-LS) haem, while Fe^{2+}AHb2 is fully 6c-LS. The CO binding kinetics are substantially different, reflecting the distribution between penta- and hexacoordinated species, and indicating that protein dynamics and ligand migration pathways are very specific for each of the two proteins. In particular, the very small, non-exponential geminate rebinding observed for AHb1 suggests that the distal haem cavity is connected to the bulk solution *via* a relatively open channel. On the other hand, the large, temperature dependent geminate rebinding observed for AHb2 suggests a major role of protein dynamics in the ligand migration from the distal cavity to the solvent.

The minimal model which is necessary to account for the observed kinetics is sketched in Scheme 1 and requires competitive binding between the exogenous (CO) and the endogenous (His E7) ligands.[27,71–76] The differential equations associated with Scheme 1 were solved numerically and the microscopic rate constants were obtained by a simultaneous fit to stopped flow and flash photolysis data at the same temperature.[69] This global analysis was repeated at several CO concentrations.

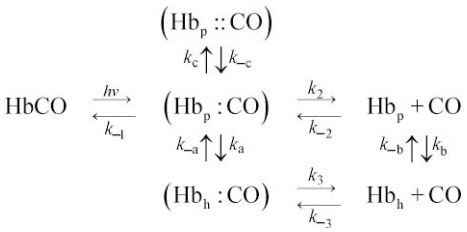

Scheme 1 Relevant chemical equilibria for the reaction of CO with AHb1 and AHb2 (Hb) to form the CO complex (HbCO). Penta- and hexacoordinated species are indicated by the suffix p and h, respectively. ($Hb_{p,h}$:CO) indicates primary docking sites with CO still inside the distal pocket, while (Hb_p::CO) indicates a site in which the photodissociated ligand is docked into an internal hydrophobic cavity, accessible from the primary docking site.

No evidence of structural relaxation affecting ligand binding kinetics was evident from the rebinding curves, and the competitive ligand binding model could successfully reproduce the rebinding kinetics under all experimental conditions.

In order to gain insight into the role played by the protein dynamics and the hydrophobic cavities in the ligand binding properties, we have encapsulated CO complexes of both proteins in silica gels. As already observed for other proteins, the encapsulation in silica gel affects the protein dynamics to an extent which is strongly dependent on the structural and dynamical properties of the protein under investigation.

The CO binding curves to AHb1, reported in Fig. 3, give clear evidence that protein dynamics does not affect substantially the kinetics in aqueous solutions at room temperature.[69] The model of the protein structure, obtained using homology modelling calculations with rice Hb as a template, suggested the existence of an open tunnel connecting the distal cavity with the solvent, thus

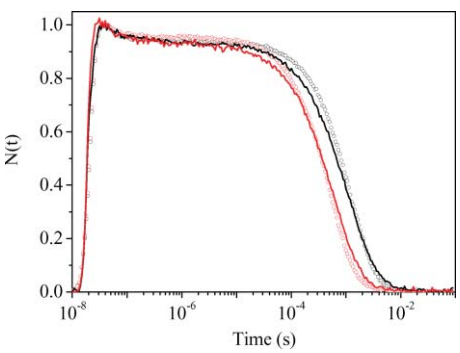

Fig. 3 Ligand binding kinetics to AHb1 solutions (circles) and gels (lines) at 10 °C (black curves) and 30 °C (red curves).

leaving an open channel which allows easy exchange of ligands between the interior and the exterior of the protein. The distal cavity is connected to other cavities into which the ligand can dock temporarily, as suggested by the non-exponential geminate phase.[69]

Fig. 3 compares the CO binding kinetics to AHb1 solutions (circles) and gels (lines) at two different temperatures, showing that the gel structure has little effect, if any, on the ligand binding kinetics. The geminate phase is essentially identical, both in amplitude and rate. The only difference which is evident in the traces is a slightly broader bimolecular phase in the gel sample, which will be discussed below.

When AHb2 is encapsulated in silica gel, the geminate rebinding becomes dramatically larger, with little effects on the apparent rate constant of the kinetics (Fig. 4). The geminate rebinding to AHb2 occurs with a single exponential decay, with a lifetime at the limit of the experimental resolution (about 10 ns). Although the kinetic trace hints to a second decay on shorter time scale, it is not possible to investigate it with the necessary accuracy. Picosecond time resolution would be necessary to better appreciate the existence of a second kinetic phase in this time range.

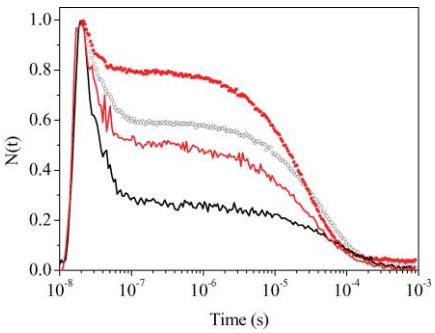

Fig. 4 Ligand binding kinetics to AHb2 solutions (circles) and gels (lines) at 10 °C (black curves) and 30 °C (red curves). The noise at $t \approx 80$ ns in the gel samples is due to an acoustic artefact caused by the shock wave generated by the intense laser pulse.

The case of AHb2 is paradigmatic, as it clearly shows how gel encapsulation can affect reactions which are strongly dependent on protein dynamics. The structure obtained by homology modelling showed no obvious connection between the distal pocket and the solvent, thus suggesting that the role of the protein dynamics is fundamental in regulating the exchange of the ligand. Accordingly, the fraction of photodissociated ligands escaping the protein matrix decreases upon increase of the constraints exerted on the protein at constant temperature.[2] This fact is a strong indication that motions at the protein surface, which are strongly damped in a viscous surrounding, are involved in the escape process. The traces shown in Fig. 4 also suggest that in the competition with the endogenous ligand, CO is favoured when the protein is inside the gel, as can be seen from the smaller residual absorbance at 1 ms.

Time-resolved spectra confirm the role of the endogenous ligand as a competitor of CO after laser photolysis

Time-resolved absorbance spectra following laser flash photolysis add strong support to the existence of competition between CO and the internal His ligand. Fig. 5 shows the first two spectral components and the time evolution of the amplitudes of each component, obtained from SVD analysis of the time-resolved transient spectra (not shown) measured after nanosecond photolysis of COAHb1 and COAHb2 solutions at room temperature. The first component is associated with the spectral change between the carboxy and the deoxy species, and hence tracks the ligand rebinding kinetics. The second component reflects formation of a transient species on the microsecond time scale, which then slowly decays at longer times. This intermediate is formed with higher efficiency at lower CO concentrations, as demonstrated for AHb2 by the green curves measured at 0.5 atm CO in Fig. 5. The spectral shape and the time course of the amplitudes are consistent with the intermediate being the hexacoordinated, bis-histidine species. In particular, the time course of the V_2 for both haemoglobins closely resembles the time course of the 6c-LS species we have previously observed in solution.[69] The time course of V_2 is also similar to the time evolution of the 6c-LS species reported in Fig. 6. When the CO concentration is decreased, the 6c-LS species is favoured as demonstrated for AHb2 by the green traces. The first component shows that a higher residual deoxy species content is remaining at 0.1 s after photolysis. This is confirmed by the second component, which is also enhanced under reduced CO partial pressure.

It is worthwhile mentioning that the second component in the SVD analysis represents a minor contribution. This can be understood by considering the singular values at 1 atm CO for AHb2 ($S_1 = 9.6$ and $S_2 = 0.16$), and for AHb1 ($S_1 = 26.9$ and

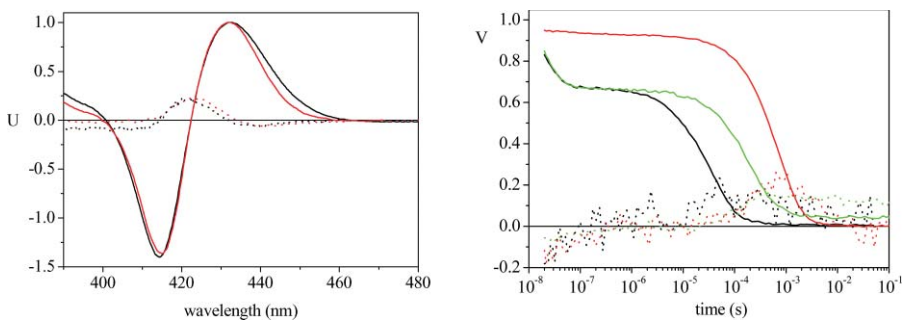

Fig. 5 Left. Comparison of the first (solid lines) and the second (dotted lines) components obtained from the SVD analysis on the time-resolved spectra measured for AHb1 (red curves) and AHb2 (black curves). Spectra U_2S_2 are shown on a $\times 10$ scale. Right. Time courses of the amplitudes V_1 (solid curves) and V_2 (dotted curves) obtained for AHb1 (red curves) and AHb2 (black curves). The concentration of CO was 1 mM, and the spectra were measured at 20 °C. The green curves in the right panel are the V_1 (solid curve) and V_2 (dotted curve) measured for AHb2 at 0.5 mM CO.

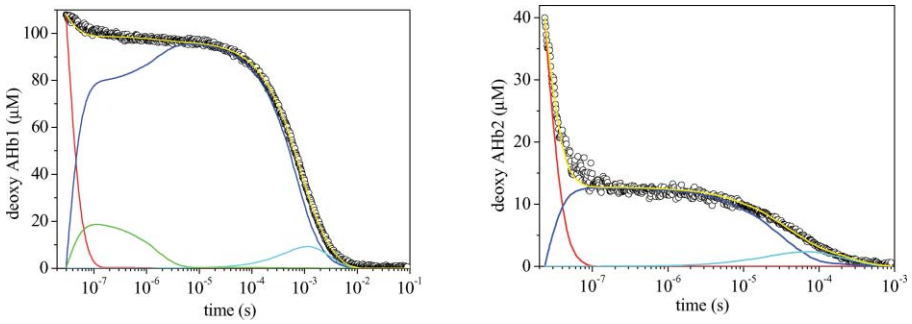

Fig. 6 Analysis of the CO binding kinetics to AHb1 (left panel) and AHb2 (right panel) gels at 1 atm CO and $T = 25$ °C. The fits (yellow lines) are superimposed to the experimental data (circles). In the figures we have also reported the time course of the other relevant species in Scheme 1: Hb_p:CO (red), Hb_p::CO (green), Hb_h (cyan), Hb_p (blue).

Table 1 Microscopic rate constants from the fit of the flash photolysis data, at 20 °C. Activation enthalpies $\Delta H^{\ddagger}$ and entropies $\Delta S^{\ddagger}$ were estimated from the linear Eyring plots for each rate constant k_i in the temperature range 10–40 °C, according to the equation: $\ln(\frac{hk_i}{k_B T}) = \frac{\Delta S^{\ddagger}}{R} - \frac{\Delta H^{\ddagger}}{RT}$ where R is the gas constant, h is the Planck's constant and k_B is the Boltzmann constant.

	AHb1			AHb2		
	k	$\Delta S^{\ddagger}$/cal mol^{-1} K^{-1}	$\Delta H^{\ddagger}$/kcal mol^{-1}	k	$\Delta S^{\ddagger}$/cal mol^{-1} K^{-1}	$\Delta H^{\ddagger}$/kcal mol^{-1}
$k_{-1}/10^6$ s^{-1}	4.8	—	—	56	—	—
$k_2/10^7$ s^{-1}	5.0	—	—	3.7	1 ± 2	7.4 ± 0.5
$k_{-2}/10^7$ M^{-1} s^{-1}	1.4	3 ± 6	9 ± 2	4.9	18 ± 1	12.1 ± 0.4
k_b/s^{-1}	320	-30 ± 5	5 ± 1	14000	-15 ± 6	7 ± 2
k_{-b}/s^{-1}	130	-32 ± 7	5 ± 2	15000	-7 ± 6	10 ± 2
$k_c/10^7$ s^{-1}	1.0	—	—	—	—	—
$k_{-c}/10^7$ s^{-1}	0.08	—	—	—	—	—

$S_2 = 0.4$). The lower S values for AHb2 at 1 atm CO are responsible for the worse signal/noise ratio which is evident in the plot of the V (black curves in Fig. 5). A slight improvement in the quality of the retrieved data for AHb2 was observed at 0.5 atm CO. Under these conditions $S_1 = 11.3$ and $S_2 = 0.8$.

Analysis of CO rebinding kinetics shows the effect of the gel on the rate constants

The analysis with the differential equations reproduces quite accurately the rebinding curves for both proteins in the investigated temperature range (10–40 °C), as previously observed in solution.[69] Sample fits for the rebinding kinetics to AHb1 and AHb2 gels at 20 °C and 1 atm CO are shown in Fig. 6, along with the time course of the various species (Scheme 1). The fit fails to reproduce the kinetic trace accurately only in the geminate phase, where structural relaxation may occur to some extent. The rate constants at 20 °C are reported in Table 1 along with the activation parameters. Several of the microscopic rate constants show similar values to the ones determined in solution,[69] with the very important exception of the rates for binding and dissociation of the endogenous ligand. The gel structure seems to speed up the reactions with the endogenous ligand for both proteins, leading to a 10-fold enhancement for AHb1 and a 50- to 100-fold increase for AHb2. The values of the rate constants k_b and k_{-b} suggest that, when embedded in the gel structure, an equilibrium between 5c-HS and 6c-LS species is observed for both proteins in their Fe^{2+} deoxy states.

The enthalpic barriers for binding of the endogenous ligand are decreased substantially for AHb1, and slightly less for AHb2. The major change seems to be on the entropic terms of the barriers, which become negative for both proteins. However, the large error bars require further investigations on these parameters. The entry/exit rates for the secondary docking site in AHb1 are two-fold smaller than the corresponding values in solution. Finally, the three-fold increase in the rate k_{-1} for AHb2 explains the enhanced amplitude of the geminate rebinding phase.

Analysis with the MEM confirms the qualitative picture emerging from the kinetic analysis

The existence of specific kinetic phases and the different role played by protein dynamics can be further appreciated by considering the lifetime distributions associated with the rebinding curves determined by the MEM. The analysis of the CO rebinding kinetics to AHb1 solutions using the MEM, reported in Fig. 7, highlights a small geminate phase with a barely detectable bimodal shape at 10 °C, with peaks at $\log(\tau) = -7.56$ and -6.56. The sharp band observed at $\log(\tau) = -2.9$ (at 10 °C) is due to the diffusion mediated bimolecular reaction.

The lifetime distributions observed for the AHb1 gels are broader than the corresponding distributions determined for the samples in solution (Fig. 7). It is difficult to attribute the broadening to a specific effect, although several sources may contribute to some extent. The gel structure may impose some constraints on the structural relaxation leading to the competitive

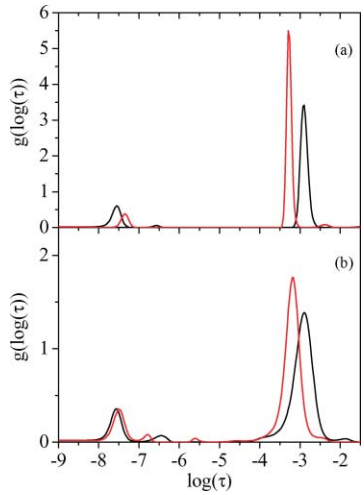

Fig. 7 Lifetime distributions obtained from the MEM for AHb1 solutions (a) and gels (b) at 10 °C (black lines) and 30 °C (red lines). Please note the different vertical axis for the two plots, due to the much sharper distribution observed for AHb1 solutions.

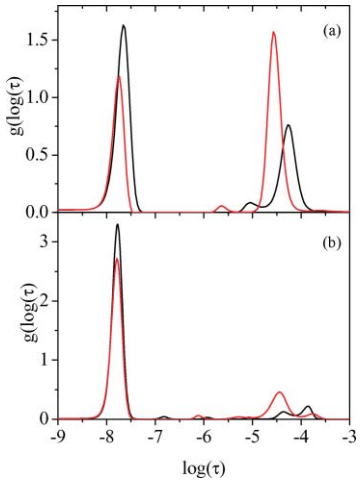

Fig. 8 Lifetime distributions obtained from the MEM for AHb2 solutions (a) and gels (b) at 10 °C (black lines) and 30 °C (red lines).

binding of the distal His and, thus, to an extended kinetics. It is also not possible to exclude structural heterogeneity due to trapping of slightly different conformations of AHb1, characterized by different binding rate constants.

Although the geminate phase appears to be scarcely affected by the gel, some specific features can be recognized. The dominant peak undergoes a less pronounced shift with temperature of its position in the gel ($\log(\tau) \approx -7.56$ at 10 °C, $\log(\tau) \approx -7.50$ at 30 °C) than in the solution ($\log(\tau) \approx -7.56$ at 10 °C, $\log(\tau) \approx -7.35$ at 30 °C). A secondary geminate band is more clearly distinguishable and shows a clearer temperature dependence in the AHb1 gel. This suggests that, even if the effects are small, migration to the secondary docking site is enhanced when AHb1 is in the gel, mostly due to the lower escape rate (k_{-c}, see Table 1). On longer time scales, three distinct peaks can be distinguished in the broad band, which can be associated with the binding of the endogenous His (shoulder at $\log(\tau) \approx -4.0$ at $T = 10$ °C), binding to the 5c-HS species (peak at $\log(\tau) \approx -2.9$), and detachment of endogenous ligand replaced by CO (small peak at $\log(\tau) \approx -1.9$). No such clear separation of the kinetic events is apparent from the solution data, the only evidence being a minor band at $\log(\tau) = -2.38$ in the 30 °C data, possibly arising from His deligation.

When we consider the effect of the gel on the CO rebinding kinetics to AHb2, we face a completely different situation. The gel exerts a very remarkable effect on the ligand rebinding, with the geminate phase being strongly enhanced in the gel. The lifetime distribution for the geminate phase in the gel becomes very sharp and narrow, in agreement with the almost perfect single exponential decay observed for these samples. As observed for AHb1 gels, the peak position of the geminate phase, observed at $\log(\tau) = -7.77$ at 10 °C, is scarcely affected by temperature (Fig. 8(b)), while the corresponding band in solution shows a normal thermal activation (Fig. 8(a)). No evidence of distinct geminate phases appears from the MEM distributions, showing that, under the present experimental conditions, no docking sites contribute to modulate the rebinding kinetics. The peaks in the microsecond range are too small to be safely attributed to a specific process and could simply reflect some noise. It is possible to recognize the His binding process in the lifetime distributions of solution samples, giving rise to a small minor peak at $\log(\tau) = -5$ at 10 °C. The bands at longer times could be due to binding to pentacoordinated haem and to His replacement by CO, respectively.

Conclusions

Several recent findings have fostered renewed interest in nanosecond laser flash photolysis of haem proteins. The interest of current research is mostly focused on the understanding of the mechanisms of ligand migration inside the matrix of the protein and its relationship with structural relaxation and protein dynamics. The availability of high resolution structures for many proteins has provided a tremendous input of information for the interpretation of previously puzzling experimental results. The existence of hydrophobic cavities capable of trapping temporarily the photodissociated ligands is now accepted as one of the reasons leading to the observed complex kinetic patterns in laser flash photolysis experiments under high viscosity. For instance, this finding explained the inverse temperature effects on rebinding kinetics at low temperatures. The role of these cavities as possible docking sites for a secondary metabolite, is at the moment only postulated in some cases. In the case on neuroglobin,[77] truncated haemoglobins[52] and, possibly, myoglobin,[50] the metabolism of NO to nitrate seems to be accomplished through docking of NO in one of these cavities, until oxygen is bound to the haem Fe. This hypothesis highlighted the possible existence of multiple functions for the same structure, with a previously unsuspected versatility of these proteins. The interplay between protein dynamics and ligand reactivity is still a hot topic for biophysical studies, as demonstrated by the fact that it was not until a couple of years ago that a model merging ligand migration and structural relaxation was proposed to explain CO rebinding kinetics to myoglobin.[33,66]

After many years of investigation on haem proteins, surprises do not seem to have an end.

Acknowledgements

The authors acknowledge MIUR (PRIN2004) for financial support. P. Dominici is kindly acknowledged for the AHb1 and AHb2 samples. P. J. Steinbach is kindly acknowledged for the use of MemExp.

References

1 R. H. Austin, K. W. Beeson, L. Eisenstein, H. Frauenfelder and I. C. Gunsalus, Dynamics of ligand binding to myoglobin, *Biochemistry*, 1975, **14**, 5355–5373.
2 D. Beece, L. Eisenstein, H. Frauenfelder, D. Good, M. C. Marden, L. Reinisch, A. H. Reynolds, L. B. Sorensen and K. T. Yue, Solvent Viscosity and Protein Dynamics, *Biochemistry*, 1980, **19**, 5147–5157.
3 W. Doster, D. Beece, S. F. Bowne, E. E. DiIorio, L. Eisenstein, H. Frauenfelder, L. Reinisch, E. Shyamsunder, K. H. Winterhalter and K. T. Yue, Control and pH Dependence of Ligand Binding to Heme Proteins, *Biochemistry*, 1982, **21**, 4831–4839.
4 E. R. Henry, J. H. Sommer, J. Hofrichter and W. A. Eaton, Geminate Recombination of Carbon Monoxide to Myoglobin, *J. Mol. Biol.*, 1983, **166**, 443–451.
5 A. Ansari, J. Berendzen, S. F. Bowne, H. Frauenfelder, I. E. T. Iben, T. B. Sauke, E. Shyamsunder and R. D. Young, *Biochemistry*, 1985, **82**, 5000–5004.
6 V. Srajer, L. Reinisch and P. M. Champion, Protein Fluctuations, Distributed Coupling, and the Binding of Ligands to Heme Proteins, *J. Am. Chem. Soc.*, 1988, **110**, 6656–6670.
7 P. J. Steinbach, Ligand binding to heme proteins: connection between dynamics and function, *Biochemistry*, 1991, **30**, 3988–4001.
8 A. Ansari, C. M. Jones, E. R. Henry, J. Hofrichter and W. Eaton, The Role of Solvent Viscosity in the Dynamics of Protein Conformational Changes, *Science*, 1992, **256**, 1796–1798.
9 W. D. Tian, J. T. Sage, V. Srajer and P. M. Champion, Relaxation dynamics of myoglobin in solution, *Phys. Rev. Lett.*, 1992, **68**, 408–411.
10 F. Post, W. Doster, G. Karvounis and M. Settles, Structural relaxation and nonexponential kinetics of CO binding to horse myoglobin. Multiple flash photolysis experiments, *Biophys. J.*, 1993, **64**, 1833–1842.
11 A. Ansari, C. M. Jones, E. R. Henry, J. Hofrichter and W. Eaton, Conformational Relaxation and Ligand Binding in Myoglobin, *Biochemistry*, 1994, **33**, 5128–5145.
12 E. Chen, R. A. Goldberg and D. S. Kliger, Nanosecond time-resolved spectroscopy of biomolecular processes, *Annu. Rev. Biophys. Biomol. Struct.*, 1997, **26**, 327–355.
13 R. M. Esquerra, R. A. Goldbeck, D. B. Kim-Shapiro and D. S. Kliger, Spectroscopic evidence for nanosecond protein relaxation after photodissociation of myoglobin–CO., *Biochemistry*, 1998, **37**, 17527–17536.
14 T. Kleinert, W. Doster, H. Leyser, W. Petry, V. Schwarz and M. Settles, Solvent Composition and Viscosity Effects on the Kinetics of CO Binding to Horse Myoglobin, *Biochemistry*, 1998, **37**, 717–733.
15 B. H. McMahon, B. P. Stojkovic, P. J. Hay, R. L. Martin and A. E. Garcia, Microscopic model of carbon monoxide binding to myoglobin, *J. Chem. Phys.*, 2000, **113**, 6831–6850.
16 J. Hofrichter, J. H. Sommer, E. R. henry and W. A. Eaton, Nanosecond absorption spectroscopy of hemoglobin: Elementary processes in kinetic cooperativity, *Proc. Natl. Acad. Sci. U. S. A.*, 1983, **80**, 2235–2239.
17 L. P. Murray, J. Hofrichter, E. R. Henry and W. A. Eaton, Time-resolved optical spectroscopy and structural dynamics following photodissociation of carbonmonoxyhemoglobin, *Biophys. Chem.*, 1988, **29**, 63–76.
18 L. P. Murray, J. Hofrichter, E. R. Henry, M. Ikeda-Saito, K. Kitagishi, T. Yonetani and W. A. Eaton, The effect of quaternary structure on the kinetics of conformational changes and nanosecond rebinding of carbon monoxide to hemoglobin, *Proc. Natl. Acad. Sci. U. S. A.*, 1988, **85**, 2151–2155.
19 E. W. Findsen, J. M. Friedman and M. R. Ondrias, Effect of Solvent Viscosity on the Heme-Pocket Dynamics of Photolyzed (Carbonmonoxy)hemoglobin, *Biochemistry*, 1988, **27**, 8719–8724.
20 C. M. Jones, A. Ansari, E. R. Henry, G. W. Christoph, J. Hofrichter and W. A. Eaton, Speed of intersubunit communication in proteins, *Biochemistry*, 1992, **31**, 6692–6702.
21 E. R. Henry, C. M. Jones, J. Hofrichter and W. A. Eaton, Can a two-state MWC allosteric model explain hemoglobin kinetics?, *Biochemistry*, 1997, **36**, 6511–6528.
22 S. C. Bjorling, R. A. Goldbeck, S. J. Paquette, S. J. Milder and D. S. Kliger, Allosteric Intermediates in Hemoglobin. 1. Nanosecond Time-Resolved Circular Dichroism Spectroscopy, *Biochemistry*, 1996, **35**, 8619–8627.
23 R. A. Goldbeck, S. J. Paquette, S. C. Björling and D. S. Kliger, Allosteric Intermediates in Hemoglobin. 2. Kinetic Modeling of HbCO Photolysis, *Biochemistry*, 1996, **35**, 8628–8639.
24 R. M. Esquerra, R. A. Goldbeck, S. H. Reaney, A. M. Batchelder, Y. Wen, J. W. Lewis and D. S. Kliger, Multiple Geminate Ligand Recombinations in Human Hemoglobin, *Biophys. J.*, 2000, **78**, 3227–3239.
25 R. A. Goldbeck, S. J. Paquette and D. S. Kliger, The Effect of Water on the Rate of Conformational Change in Protein Allostery, *Biophys. J.*, 2001, **81**, 2919–2934.
26 S. Dewilde, L. Kiger, T. Burmester, T. Hankeln, V. Baudin-Creuza, T. Aerts, M. C. Marden, R. Caubergs and L. Moens, Biochemical Characterization and Ligand Binding Properties of Neuroglobin, a Novel Member of the Globin Family, *J. Biol. Chem.*, 2001, **276**, 38949–38955.
27 J. M. Kriegl, A. J. Bhattacharyya, K. Nienhaus, P. Deng, O. Minkow and G. U. Nienhaus, Ligand binding and protein dynamics in neuroglobin, *Proc. Natl. Acad. Sci. U. S. A.*, 2002, **99**, 7992–7997.
28 S. Bettati, B. Pioselli, B. Campanini, C. Viappiani and A. Mozzarelli, Protein-Doped Nanoporous Silica Gels, in *Encyclopedia of Nanoscience and Nanotechnology*, ed. H. S. Nalwa, American Scientific Publishers, Stevenson Ranch, California, 2004, pp. 81–103.
29 C. Viappiani, S. Bettati, S. Bruno, L. Ronda, S. Abbruzzetti, A. Mozzarelli and A. W. Eaton, New insights into allosteric mechanisms from trapping unstable protein conformations, *Proc. Natl. Acad. Sci. U. S. A.*, 2004, **101**, 14414–14419.
30 S. Sottini, S. Abbruzzetti, C. Viappiani, S. Bettati, L. Ronda and A. Mozzarelli, Evidence for two geminate rebinding states following laser photolysis of R state hemoglobin encapsulated in wet silica gels, *J. Phys. Chem. B*, 2005, **109**, 11411–11413.
31 S. Sottini, S. Abbruzzetti, C. Viappiani, L. Ronda and A. Mozzarelli, Determination of microscopic rate constants for CO binding and migration in myoglobin encapsulated in silica gels, *J. Phys. Chem. B*, 2005, **109**, 19523–19528.
32 S. Sottini, S. Abbruzzetti, F. Spyrakis, S. Bettati, L. Ronda, A. Mozzarelli and C. Viappiani, Geminate rebinding in R state hemoglobin: kinetic and computational evidence for multiple hydrophobic pockets, *J. Am. Chem. Soc.*, 2005, **127**, 17427–17432.
33 D. Dantsker, U. Samuni, J. M. Friedman and N. Agmon, A hierarchy of functionally important relaxations within myoglobin based on solvent effects, mutations and kinetic model, *Biochim. Biophys. Acta*, 2005, **1749**, 234–251.
34 U. Samuni, D. Dantsker, A. Ray, J. B. Wittenberg, B. A. Wittenberg, S. Dewilde, L. Moens, Y. Ouellet, M. Guertin and J. M. Friedman, Kinetic Modulation in Carbonmonoxy Derivatives of Truncated Hemoglobins. The role of distal heme pocket residues and extended apolar tunnel, *J. Biol. Chem.*, 2003, **278**, 27241–27250.
35 D. Dantsker, U. Samuni, A. J. Friedman, M. Yang, A. Ray and J. M. Friedman, Geminate Rebinding in Trehalose-glass Embedded Myoglobins Reveals Residue-specific Control of Intramolecular Trajectories, *J. Mol. Biol.*, 2002, **315**, 239–251.
36 S. Abbruzzetti, C. Viappiani, S. Bruno, S. Bettati, M. Bonaccio and A. Mozzarelli, Functional Characterization of Heme Proteins Encapsulated in Wet Nanoporous Silica Gels, *J. Nanosci. Nanotech.*, 2001, **1**, 407–415.
37 S. Abbruzzetti, C. Viappiani, S. Bruno and A. Mozzarelli, Enhanced geminate ligand rebinding upon photo-dissociation of silica gel-embedded myoglobin–CO, *Chem. Phys. Lett.*, 2001, **346**, 430–436.
38 M. Brunori and Q. H. Gibson, Cavities and packing defects in the structural dynamics of myoglobin, *EMBO Rep.*, 2001, **2**, 674–679.
39 E. E. Scott and Q. H. Gibson, Ligand Migration in Sperm Whale Myoglobin, *Biochemistry*, 1997, **36**, 11909–11917.
40 E. E. Scott, Q. H. Gibson and J. S. Olson, Mapping the Pathways for O_2 Entry Into and Exit from Myoglobin, *J. Biol. Chem.*, 2001, **276**, 5177–5188.

41 C. Tetreau, Y. Blouquit, E. Novikov, E. Quiniou and D. Lavalette, Competition with Xenon Elicits Ligand Migration and Escape Pathways in Myoglobin, *Biophys. J.*, 2004, **86**, 435–447.
42 R. F. J. Tilton, I. D. J. Kuntz and G. A. Petsko, Cavities in Proteins: Structure of a Metmyoglobin–Xenon Complex Solved to 1.9 Å, *Biochemistry*, 1984, **23**, 2849–2857.
43 I. Schlichting, J. Berendzen, G. N. Phillips and R. M. Sweet, Crystal structure of photolysed carbonmonoxy–myoglobin, *Nature*, 1994, **371**, 808–812.
44 A. Ostermann, R. Washipky, F. G. Parak and G. U. Nienhaus, Ligand binding and conformational motions in myoglobin, *Nature*, 2000, **404**, 205–208.
45 K. Chu, J. Vojtchovsky, B. H. McMahon, R. M. Sweet, J. Berendzen and I. Schlichting, Structure of a ligand-binding intermediate in wild-type carbonmonoxy myoglobin, *Nature*, 2000, **403**, 921–923.
46 V. Srajer, Z. Ren, T. Y. Teng, M. Schmidt, T. Ursby, D. Bourgeois, C. Pradervand, W. Schildkamp, M. Wulff and K. Moffat, Protein Conformational Relaxation and Ligand Migration in Myoglobin: A Nanosecond to Millisecond Molecular Movie from Time-Resolved Laue X-ray Diffraction, *Biochemistry*, 2001, **40**, 13802–13815.
47 D. Bourgeois, B. Vallone, F. Schotte, A. Arcovito, A. E. Miele, G. Sciara, M. Wulff, P. Anfinrud and M. Brunori, Complex landscape of protein structural dynamics unveiled by nanosecond Laue crystallography, *Proc. Natl. Acad. Sci. U. S. A.*, 2003, **100**, 8704–8709.
48 F. Schotte, M. Lim, T. A. Jackson, A. V. Smirnov, J. Soman, J. S. Olson, G. N. P. Jr., M. Wulff and P. A. Anfinrud, Watching a Protein as it Functions with 150-ps Time-Resolved X-ray Crystallography, *Science*, 2003, **300**, 1944–1947.
49 D. Bourgeois, B. Vallone, A. Arcovito, G. Sciara, F. Schotte, P. A. Anfinrud and M. Brunori, Extended subnanosecond structural dynamics of myoglobin revealed by Laue crystallography, *Proc. Natl. Acad. Sci. U. S. A.*, 2006, **103**, 4924–4929.
50 M. Brunori, Nitric oxide moves myoglobin centre stage, *Trends Biochem. Sci.*, 2001, **26**, 209–210.
51 A. Pesce, M. Bolognesi, A. Bocedi, P. Ascenzi, S. Dewilde, L. Moens, T. Hankeln and T. Burmester, Neuroglobin and cytoglobin Fresh blood for the vertebrate globin family, *EMBO Rep.*, 2002, **3**, 1146–1151.
52 A. Bidon-Chanal, M. A. Martí, A. Crespo, M. Milani, M. Orozco, M. Bolognesi, F. J. Luque and D. A. Estrin, Ligand-induced dynamical regulation of NO conversion in Mycobacterium tuberculosis truncated-hemoglobin-N, *Proteins*, 2006, **64**, 457–464.
53 G. Cosa and J. C. Scaiano, Laser Techniques in the Study of Drug Photochemistry, *Photochem. Photobiol.*, 2004, **80**, 159–174.
54 R. Bonneau, J. Wirz and A. D. Zuberbuehler, Methods for the analysis of transient absorbance data, *Pure Appl. Chem.*, 1997, **69**, 979–992.
55 C. Tetreau and D. Lavalette, Dominant features of protein reaction dynamics: Conformational relaxation and ligand migration, *Biochim. Biophys. Acta*, 2005, **1724**, 411–424.
56 A. Banderini, S. Sottini and C. Viappiani, Method for detecting extended real-time kinetics in nanosecond laser flash photolysis experiments, *Rev. Sci. Instrum.*, 2004, **75**, 2257–2261.
57 S. Abbruzzetti, S. Sottini, C. Viappiani and J. E. T. Corrie, Kinetics of proton release after flash photolysis of 1-(2-nitrophenyl)ethyl sulfate (caged sulfate) in aqueous solutions, *J. Am. Chem. Soc.*, 2005, **127**, 9865–9874.
58 A. Fenster, J. C. LeBlanc, W. B. Taylor and H. E. Jones, Linearity and fatigue in photomultipliers, *Rev. Sci. Instrum.*, 1973, **44**, 689–694.
59 C. Viappiani, S. Abbruzzetti, J. R. Small, L. J. Libertini and E. W. Small, An experimental methodology for measuring volume changes in proton transfer reactions in aqueous solutions, *Biophys. Chem.*, 1998, **73**, 13–22.
60 S. Abbruzzetti, C. Viappiani, J. R. Small, L. J. Libertini and E. W. Small, Kinetics of histidine deligation from the heme in GuHCl unfolded Fe(III) cytochrome c studied by a laser induced pH-jump technique, *J. Am. Chem. Soc.*, 2001, **123**, 6649–6653.
61 F. Librizzi, C. Viappiani, S. Abbruzzetti and L. Cordone, Residual water modulates the dynamics of the protein and of the external matrix in "*trehalose coated*" MbCO: an infrared and flash photolysis study, *J. Chem. Phys.*, 2002, **116**, 1193–1200.
62 C. Viappiani, S. Abbruzzetti, S. Bologna, B. Campanini, S. Bettati and A. Mozzarelli, Kinetics of acid-induced structural changes in GFPmut2 chromophore, *Biophys. J.*, 2003, **84**, 341A.
63 L. Cordone, G. Cottone, S. Giuffrida, G. Palazzo, G. Venturoli and C. Viappiani, Internal dynamics and protein-matrix coupling in trehalose-coated proteins, *Biochim. Biophys. Acta*, 2005, **1749**, 252–281.
64 J. M. Kriegl, F. K. Forster and G. U. Nienhaus, Charge Recombination and Protein Dynamics in Bacterial Photosynthetic Reaction Centers Entrapped in a Sol-Gel Matrix, *Biophys. J.*, 2003, **85**, 1851–1870.
65 E. R. Henry and J. Hofrichter, Singular value decomposition: application to analysis of experimental data, in *Numerical computer methods*, ed. L. Brand and M. L. Johnson, Academic Press, Inc., San Diego, 1992, pp. 129–192.
66 N. Agmon, Coupling of Protein Relaxation to Ligand Binding and Migration in Myoglobin, *Biophys. J.*, 2004, **87**, 1537–1543.
67 P. J. Steinbach, R. Ionescu and C. R. Matthews, Analysis of Kinetics Using a Hybrid Maximum-Entropy/Nonlinear-Least-Squares Method: Application to Protein Folding, *Biophys. J.*, 2002, **82**, 2244–2255.
68 P. J. Steinbach, Inferring Lifetime Distributions from Kinetics by Maximizing Entropy Using a Bootstrapped Model, *J. Chem. Inf. Comput. Sci.*, 2002, **42**, 1476–1478.
69 S. Bruno, S. Faggiano, F. Spyrakis, A. Mozzarelli, S. Abbruzzetti, E. Grandi, C. Viappiani, A. Feis, S. Mackowiak, G. Smulevich, E. Cacciatori and P. Dominici, The reactivity with CO of AHb1 and AHb2 from *Arabidopsis thaliana* is controlled by the distal His E7 and internal hydrophobic cavities, 2006, submitted.
70 N. Shibayama and S. Saigo, Fixation of the Quaternary Structures of Human Adult Haemoglobin by Encapsulation in Transparent Porous Silica Gels, *J. Mol. Biol.*, 1995, **251**, 203–209.
71 M. S. Hargrove, A Flash Photolysis Method to Characterize Hexacoordinate Hemoglobin Kinetics, *Biophys. J.*, 2000, **79**, 2733–2738.
72 J. T. I. Trent, A. N. Hvitved and M. S. Hargrove, A Model for Ligand Binding to Hexacoordinate Hemoglobins, *Biochemistry*, 2001, **40**, 6155–6163.
73 S. VanDoorslaer, S. Dewilde, L. Kiger, S. V. Nistor, E. Goovaerts, M. C. Marden and L. Moens, Nitric Oxide Binding Properties of Neuroglobin. A characterization by EPR and flash photolysis, *J. Biol. Chem.*, 2003, **278**, 4919–4925.
74 J. Uzan, S. Dewilde, T. Burmester, T. Hankeln, L. Moens, D. Hamdane, M. C. Marden and L. Kiger, Neuroglobin and Other Hexacoordinated Hemoglobins Show a Weak Temperature Dependence of Oxygen Binding, *Biophys. J.*, 2004, **87**, 1196–1204.
75 L. Kiger, J. Uzan, S. Dewilde, T. Burmester, T. Hankeln, L. Moens, D. Hamdane, V. Baudin-Creuza and M. C. Marden, Neuroglobin ligand binding kinetics, *IUBMB Life*, 2004, **56**, 709–719.
76 A. I. Ioanitescu, S. Dewilde, L. Kiger, M. C. Marden, L. Moens and S. VanDoorslaer, Characterization of Nonsymbiotic Tomato Hemoglobin, *Biophys. J.*, 2005, **89**, 2628–2639.
77 M. Brunori, A. Giuffre, K. Nienhaus, G. U. Nienhaus, F. M. Scandurra and B. Vallone, Neuroglobin, nitric oxide, and oxygen: Functional pathways and conformational changes, *Proc. Natl. Acad. Sci. U. S. A.*, 2005, **102**, 8483–8488.

